

# An Investigation of Fretting Fatigue in Marine Environments – I

## Fatigue Test Rig and Some Test Results

Masaaki Takeuchi, Yoshihide Kon, Yoshihiro Miyoshi, and Eiki Osaki

A new test rig was designed to investigate the detrimental phenomena, which were caused by the interaction of corrosion, fatigue and wear, occurring in structures in marine environments. This rig is capable of testing in seawater. The details of the test rig are shown and reliability and availability of the rig are confirmed. Fretting fatigue tests of an austenitic stainless steel (SUS304) focussing on the fretting damage occurring on a propeller tail shaft in small vessels were carried out in seawater and air. Fretting has a significant damaging effect on the stainless steel, reducing the fatigue strength from 300 MPa to 200 MPa in air and to 150 MPa at  $10^7$  cycles in seawater. The fretting fatigue behaviour in seawater can be determined as the balance of electrochemical, tribological and mechanical damaging processes.

### 1 Introduction

For the systematic development and effective use of sea and marine resources including fishery products, it is essential to establish engineering technology in constructing structures in marine environments which should be reliable over a long time. The life of structures in such a severe environment is entirely dependent on corrosion, wear and fatigue, etc. Consequently an investigation on the mechanisms of such damage and the establishment of effective preventative techniques against the damage are needed.

There have been a great deal of research on

each subject such as corrosion and corrosion-fatigue. However, there is little information on the complicated phenomena which are caused by the interaction of corrosion, fatigue and wear. Therefore the present investigation was set up.

In this paper, the details of the test rig which was designed to investigate the detrimental phenomena occurring in structures in marine environments were described. Moreover, fatigue tests focussing on the fretting damage occurring on a propeller tail shaft in a small vessel were carried out and the reliability and availability of the test rig were confirmed.

## 2 Design

### 2.1 Test rig

Although many types of test rig have been designed for wear and fatigue tests, the basic principle of the present test rig is based on the machine designed by Nishioka and Hirakawa<sup>1)</sup>.

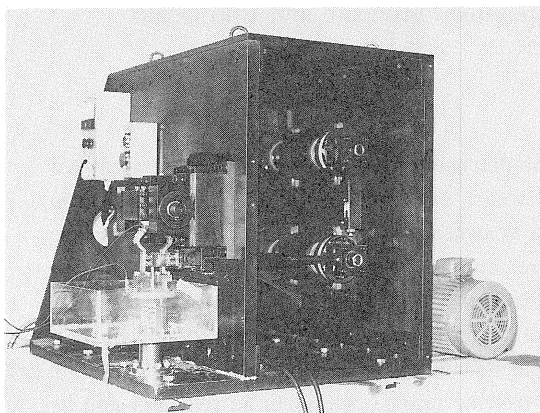


Fig. 1. A photograph of the test rig.

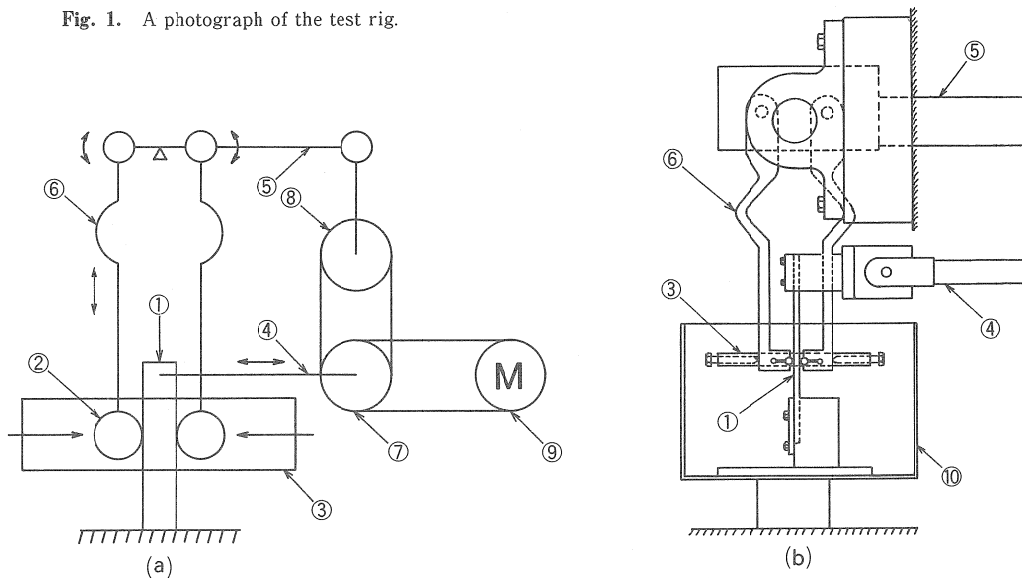


Fig. 2. A schematic diagram of the test rig (a), and details of the specimen holder part (b); ① fatigue specimen, ② fretting pad, ③ proving ring, ④ connecting rod, ⑤ fretting lever, ⑥ test piece lever, ⑦⑧ eccentric wheel, ⑨ motor, ⑩ trough.

The test rig is capable of testing wear, fatigue and fretting fatigue simultaneously or separately. The rig is improved in order to carry out the tests in a marine environment, namely seawater. Figure 1 shows a photograph of the test rig. A schematic diagram of the rig and details of the specimen holder parts are shown in Figs. 2 (a) and 2 (b) respectively. The principal performances of the rig are listed in Table 1.

One end of the fatigue specimen ①, which is flat, is fixed and the other free end is oscillated horizontally by the eccentric wheel ⑦ through the connecting rod ④. The fatigue specimen is clamped with two fretting pads ② by the proving ring ③. The fretting pads ②, which are cylindrical, fixed on the test piece levers ⑥ which are connected to another eccentric wheel ⑧ give vertical reciprocating frictional force to the contacting surfaces. Two eccentric wheels are connected with a toothed belt and are driven by a

**Table 1.** The principal performances of the test rig

Clamping load (max.)	1000 N
Eccentricity of wheel (max.)	16 mm
Frequency of alternating stress	1~20 Hz
Variable speed motor	2.2 kW, 1780 rpm
Environments	air, seawater

variable speed motor ⑨. A poly methyl methacrylate trough ⑩ is made to carry out the tests in seawater. The specimen can, therefore, be subjected to both fretting and fatigue simultaneously in seawater or air.

## 2.2 Normal load control

As shown in Fig. 2(b), the normal load is applied to the fretting contacts by the proving ring which enables clamping pressure to be adjusted. The proving ring is strain-gauged to determine the applied normal load. The relation between the strain of the proving ring and the applied load has been obtained beforehand. The magnitude of the load can be adjusted by turning the nut. The strain gauges are connected with an amplifier and the applied normal load is indicated on the normal load display.

## 2.3 Relative slip amplitude and frequency control

The amplitude of fretting oscillation can be adjusted in the range of 0 to 650  $\mu\text{m}$  by the eccentric wheel. As shown in Fig. 3, the rela-

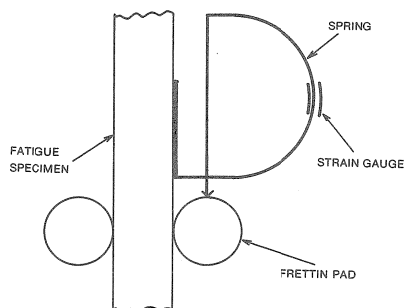


**Fig. 3.** Details of the relative slip amplitude measurement.

tive slip amplitude can be measured by a specially made spring type slip amplitude detector on which the strain gauges are attached. The frequencies of alternating bending stress and fretting oscillation can be set up in the range of 1 to 20 Hz by the motor.

## 2.4 Coefficient of friction

The test piece lever is strain-gauged to measure the tangential force between the fatigue specimen and the fretting pad. The tangential force is monitored throughout the tests. Figure 4 shows the relation between the coefficient of friction (in maximum frictional force) and relative

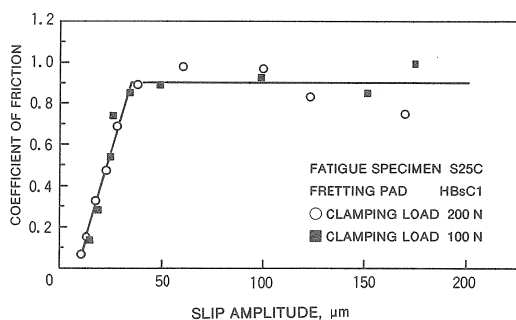


**Fig. 4.** The relation between the coefficient of friction and relative slip amplitude at a frequency of 10 Hz.

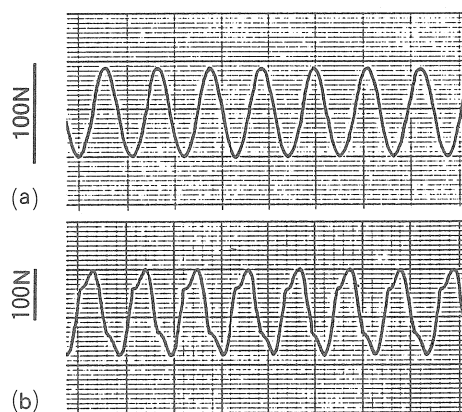


**Fig. 5.** An example of the tangential force traces at a clamping load of 200 N; (a) slip amplitude 25  $\mu\text{m}$ , (b) slip amplitude 100  $\mu\text{m}$ .

slip amplitude at the clamping loads of 100 and 200 N. The result in Fig. 4 indicates that the transition from partial slip to full slip occurs at a slip amplitude of  $40 \mu\text{m}$ . Figure 5 shows the tangential force traces at slip amplitudes of 25(a) and  $100 \mu\text{m}$ (b).

### 3 Experimental

The fatigue specimen used in the tests was an austenitic stainless steel (SUS304) which was one of the materials used for a propeller shaft in a small vessel. The fretting pad was an aluminium bronze (A1BC3) which was one of the materials used for a propeller. The mechanical properties and chemical compositions of the specimen and pad are shown in Tables 2 to 4. Figure 6 shows the details of the specimens. The fatigue specimen and the fretting pad were adraded on a silicon paper to approximately surface roughness  $R_{\text{max}} 0.2$ . All the specimens and pads were cleaned with acetone prior to the tests.

The experimental conditions were as follows; a clamping load of 260 N (the maximum Hertzian

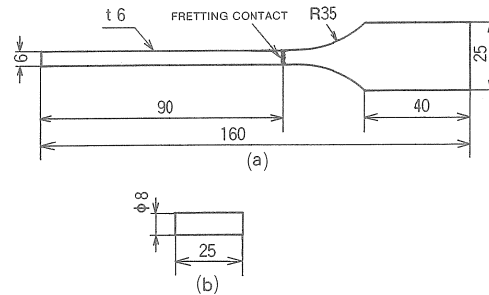


Fig. 6. Details of the fatigue specimen (a) and fretting pad (b).

contact pressure of 521 MPa and the contacting width of  $106 \mu\text{m}$ ), a frequency of 10 Hz and relative slip amplitudes of  $50 \mu\text{m}$ .

The S-N curves were determined in artificial seawater made up according to ASTM standard D1141-52 and also in air. In the tests, a teflon film sheet ( $200 \mu\text{m}$  in thickness) was inserted in one of the fretting contacts to allow the crack initiation at only one fretting contact. The bending stress at the fretting contact was obtained as follows; 1) the relation between the added static load at the free end of the specimen

Table 2. Mechanical properties

	SUS304 (Fatigue specimen)	A1BC3 (Fretting pad)
Tensile strength (MPa)	588	684
Elongation (%)	61	24
Hardness	79 (HRb)	163 (BHN)

Table 3. Chemical compositions of the fatigue specimen

	Cr	Ni	Mn	Si	C	P	S	Fe
SUS304	18.33	8.40	1.51	.62	.06	.03	.009	Bal.

Table 4. Chemical compositions of the fretting pad

	Cu	Mu	Fe	Al	Ni
A1BC3	81.23	1.12	3.94	9.04	4.49

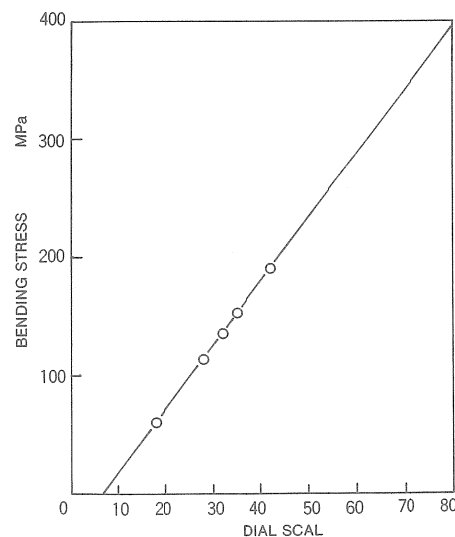


Fig. 7. The bending stress at the fretting contact vs. the dial (scal) of the eccentric wheel.

and the deflection at this point was obtained, 2) the relation between the dial (scal) of the eccentric wheel (⑦ in Fig. 2) and the value of the eccentricity of the wheel was obtained, 3) from these two relation curves, the relation between the bending stress and the dial (scal) of the eccentric wheel was determined (Fig. 7). The frictional force was monitored throughout the tests. Some of the specimens tested were examined to observe crack and wear in a scanning electron microscope.

#### 4 Results

Figure 8 shows the fatigue curves determined in seawater and air in the absence of fretting. The specimens were failed at the lower end of the parallel portion. Both curves well defined a fatigue limit at about an alternating stress of 300 MPa. It is noted that there was not any significant difference between the fatigue limit in seawater and that in air.

Figure 9 shows the fretting fatigue curves determined in seawater and air. In this case, failure always occurred at the fretting contact. The curve in air also well defined a fatigue limit at an alternating stress of 200 MPa. On the other hand, in seawater longer fatigue lives than

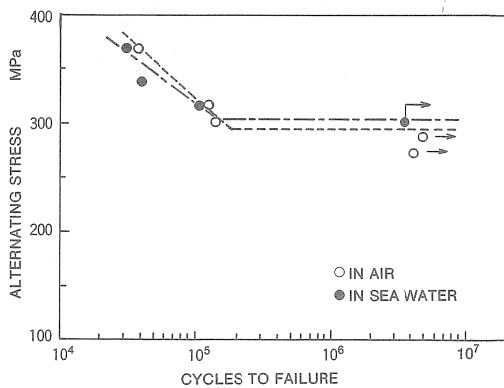


Fig. 8. Normal fatigue curves for SUS304 in seawater and air.

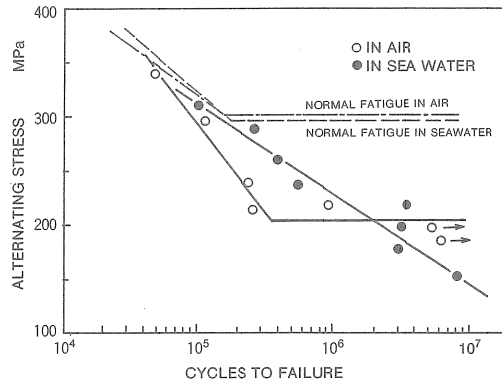


Fig. 9. Fretting fatigue curves for SUS304 in seawater and air.

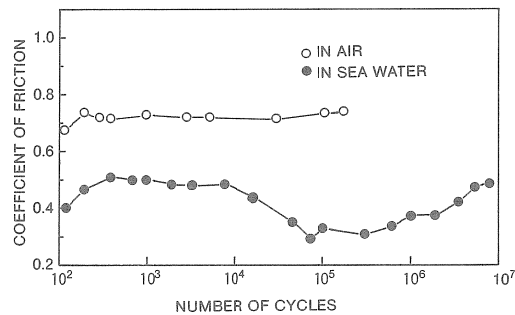


Fig. 10. The coefficient of friction vs. the number of cycles at an alternating stress of 156 MPa in seawater and 220 MPa in air.

those in air were obtained above the fatigue limit in air but the curves still fell at low stresses.

Figure 10 shows the frictional behaviour in seawater and air. The coefficient of friction increased to 0.7 within  $10^2$  cycles due to the disruption of the oxide films between the contacting surfaces and the formation of the metal to metal contact and became almost stable at 0.75. In seawater the coefficient of friction was much lower than that in air and varied in the range of 0.3 and 0.5.

Figure 11 shows the width of the fretting scar produced on each fatigue specimen plotted against the number of cycles. The width of the

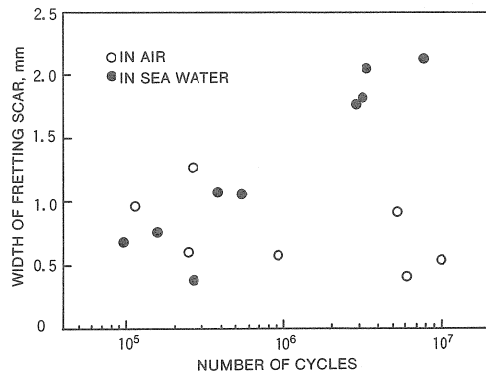


Fig. 11. The width of the fretting scar produced on each fatigue specimen plotted against the number of cycles in seawater and air.

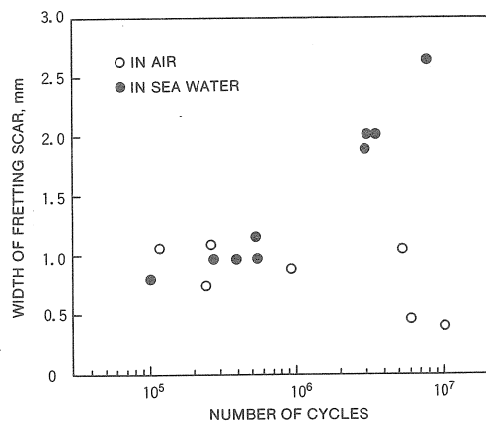


Fig. 12. The width of the fretting pad produced on each fretting pad plotted against the number of cycles in seawater and air.

scar parallel to the fretting direction was measured in an optical microscope. In air the scarring in wear was seen but did not increase with the increasing number of cycles. In seawater wear increased almost linearly according to the number of cycles. The width of the fretting scar produced on the fretting pad was plotted against the number of cycles in Fig. 12.

Figure 13 shows the appearance of the fracture in air with the fretting scar. It was appa-

rent that the crack which caused the fracture followed the left hand side of the scar. The centre of the scar was mainly compacted and smeared debris. Figure 14 is the corresponding picture of fracture in seawater at a higher magnification. Another fatigue crack was visible on the right hand side of the fractured surface and scar was free of debris. The wear debris produced by fretting occurring between the crack walls was also visible. This is due to crack closure.

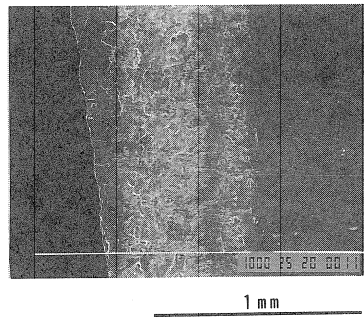


Fig. 13. SEM photograph of fracture in air; an alternating stress of 215 MPa,  $2.62 \times 10^5$  cycles to failure.

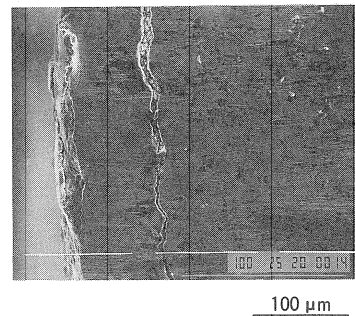


Fig. 14. SEM photograph of fracture in seawater; an alternating stress of 156 MPa,  $7.93 \times 10^6$  cycles to failure.

## 5 Discussion

The fatigue of corrosive materials such as carbon steel generally does not have a well defined fatigue limit in seawater due to the con-

tinuous dissolution of the metal<sup>2,3</sup>). On a stainless steel which is a corrosion resistant material, the fatigue strength in seawater is reduced to some extent compared with that in air but the reduction rate in the fatigue limit is not as much as that of the carbon steel<sup>2,4</sup>). Seawater with lower pH is discernibly detrimental<sup>4</sup>). However, the result in Fig. 8 shows that seawater does not have a noticeable influence on the fatigue behaviour under the present experimental conditions.

The result in Fig. 9 shows how severe is the effect of fretting on the fatigue strength of this material. The deleterious effect of fretting is more significant in seawater than in air. The reductions in fatigue strength by fretting are 35 % in air and 50 % at  $10^7$  cycles in seawater. This is due to the additional alternating shear stress<sup>5</sup>) on the fretting contact and also tribological damage<sup>6</sup>). The result in Fig. 9 also indicates that the fatigue behaviour in seawater is determined as a balance of the following processes; 1) the disruption of the oxide films, which are protective, by the mechanical action of fretting, 2) the acceleration of the electrochemical reactions (dissolution of metal) due to the direct contact of the newly formed reactive surface with an electrolyte (Fig. 11), 3) the relaxation in the contacting stress states due to wear (Figs. 11 and 12), 4) the mitigation of the mechanical action due to the lubricating effect of seawater (Fig. 10) and 5) the cooling effect of seawater at the fretting contact leading to an increase in the fatigue performance<sup>2,7</sup>).

## 6 Conclusions

A test rig has been designed to investigate tribological damage, corrosion or fatigue which may directly determine the life of the structures used in marine environments. This rig is capable of testing for various purposes such as corrosion, wear and fatigue assessments. The

details of the rig are shown.

Fretting fatigue tests of an austenitic stainless steel (SUS304) focussing on the fretting damage occurring on a propeller tail shaft in small vessels are carried out in seawater and air. The results show that 1) fretting has a significant damaging effect on the stainless steel, reducing the fatigue strength from 300 MPa to 200 MPa in air and to 150 MPa at  $10^7$  cycles in seawater, 2) the fretting fatigue behaviour in seawater can be determined as the balance of electrochemical, tribological and mechanical damaging processes.

## References

- 1) K. Nishioka and K. Hirakawa : *Trans. JSME*, **12** (50), 180-187 (1969).
- 2) Y. Gotoh and H. Ohuchida : *J. Soc. Mater. Sci.*, **35** (394), 797-803 (1986).
- 3) Y. Endo and K. Komai : *Kinzoku no fushoku hiroh to kyodo sekkei*, 1st ed., Yokendo, Tokyo, 1982, p.17.
- 4) S. Kawai, K. Kasai, and S. Kotani : *J. Soc. Mater. Sci.*, **30**(329), 173-179 (1981).
- 5) Y. Endo and H. Goto : *Wear*, **38**, 311-324 (1976).
- 6) J. Sato, M. Shima, K. Isogai, M. Takeuchi, and T. Jibiki : *Proc. 4th Inter. Symp. on Marine Engineering, MESJ, Kobe*, 1990, in press.
- 7) R. B. Waterhouse, M. K. Dutta, and P. J. Swallow : *Proc. Inter. Conf. on Mechanical Behaviour of Materials, Soc. Mater. Sci., Kyoto*, 292-298 (1972).

## 海洋環境下におけるフレッチング疲労に関する研究－I

### 試験機の試作と二三の結果

竹内正明・今 義英・三好佳広・大崎栄喜

海洋環境下における構造物では腐食，摩耗，疲労などの相互作用によって生じる損傷が問題となる。その機構の解明と防止法を研究するために，海水中で摩耗および疲労がそれぞれ独立にまたは同時に試験できる汎用性の装置を試作した。本報では，試験機の概要とその性能を示すとともに，その信頼性，有用性を確認した。また，本試験機を用いて，小型船のプロペラ軸に生じるフレッチング疲労損傷について，ステンレス鋼（SUS304）の疲労試験を海水中と大気中で行った。フレッチングは疲労強度を著しく低下させること，海水中のフレッチング疲労挙動は電気化学的，トライボロジー的および機械的損傷の均衡した結果として決定されることなどが明らかとなった。